

Protein-Lipid Interactions. Studies of the M13 Coat Protein in Dimyristoylphosphatidylcholine Vesicles Using Parinaric Acid[†]

David Kimelman,[†] Evelyn S. Tecoma,[§] Paul K. Wolber, Bruce S. Hudson,*^{||} William T. Wickner, and Robert D. Simoni*^{||}

ABSTRACT: Addition of the M13 virus coat protein to dimyristoylphosphatidylcholine vesicles decreases the amplitude of the lipid bilayer phase transition observed with parinaric acid fluorescence intensity. According to these measurements, the solid-phase bilayer is disordered by the protein, while the fluid phase is not appreciably affected. The decrease in the relative amplitude of the transition as a function of protein concentration is shown to be consistent with a perturbation of about 70 lipids by the coat protein and a preferential partitioning of *trans*-parinaric acid into the bulk bilayer rather than the perturbed annular region. The fluorescence of the single tryptophan residue of the coat protein was found to be very efficiently quenched by addition of parinaric acid. The *cis* and *trans* isomers of parinaric acid are equally efficient as quenchers at 30 °C when the bilayer is in its fluid state,

but at 10 °C the quenching by the *cis* isomer is much more efficient than for the *trans* isomer. The quenching efficiency does not depend on the coat protein concentration. These results are consistent with a perturbation of the bilayer by the coat protein at low temperature. The structure of the bilayer near the protein results in a spatial distribution of *trans*-parinaric acid such that this quencher avoids the donor protein. The intensity and partitioning/quenching behavior used to characterize the effect of the protein on the solid bilayer do not reveal any bilayer structural changes for the fluid-phase bilayer. However, fluorescence polarization measurements with parinaric acid reveal a marked decrease in the rotational mobility of the probe relative to that of the fluid bilayer. The utility of parinaric acid fluorescence methods in the study of membrane-bound proteins is emphasized.

There is considerable interest in understanding the interactions of membrane proteins with membrane lipids. It is clear that in many cases alterations of membrane lipid composition can affect the function of membrane proteins. The examination of purified membrane proteins that have been reconstituted into lipid vesicles has been particularly informative in molecular terms. Such systems permit physical analysis of highly purified components free of the complexity of the original membrane. Application of a variety of physical techniques to a number of reconstituted membrane proteins has been recently reviewed (Sandermann, 1978; Chapman, 1979).

The capsid or major coat protein (CP)¹ of the coliphage M13 can be readily incorporated into lipid vesicles, spanning the bilayer *in vitro* as it does *in vivo* (Wickner, 1975, 1976). In addition, the 5200-dalton protein contains a single tryptophan residue located in the central, hydrophobic region of the protein (Asbeck et al., 1969), which makes it ideally suited for energy transfer experiments. Previous studies (Wickner, 1976) have shown that vesicles made by a detergent dilution procedure are large, single-walled structures with coat protein

spanning the bilayer. Recently, this protein has been studied by nuclear magnetic resonance techniques (Oldfield et al., 1978; Hagen et al., 1978).

Parinaric acid (PnA, 9,11,13,15-octadecatetraenoic acid) can be used as a fluorescent probe and as the acceptor chromophore in fluorescence energy transfer studies. PnA, a naturally occurring conjugated polyene fatty acid, has been shown to be a sensitive probe of both membrane fluidity (Sklar et al., 1975, 1977a; Tecoma et al., 1977) and lipid-protein interactions (Sklar et al., 1977b; Berde et al., 1979). Some of the properties of PnA relevant to the present study include the following: (1) PnA absorption overlaps tryptophan emission; (2) the probe readily associates with lipid vesicles in a predictable orientation, without perturbing the membrane structure; (3) extremely low concentrations of PnA (<1 μ M) are sufficient to observe energy transfer; (4) the availability of both *cis*-PnA (9,11,13,15-*cis,trans,trans,cis*-octadecatetraenoic acid) and *trans*-PnA (9,11,13,15-*all-trans*-octadecatetraenoic acid) permits use of probes which are known to partition between solid- and fluid-phase lipids with different partition coefficients (Sklar et al., 1977a, 1979); (5) PnA fluorescence intensity and polarization are sensitive indicators of the state of the bilayer (Sklar et al., 1977a).

In this work we report the use of fluorescence intensity, polarization, and energy transfer measurements to determine the effect of the M13 coat protein on the structure of a lipid bilayer. Significant structural changes are observed even at low protein to lipid ratios, and a consistent structural picture can be constructed from independent measurements.

Materials and Methods

Coat protein was prepared according to Knippers & Hoffman-Berling (1966). Reconstituted vesicles were prepared

[†] From the Department of Biological Sciences (D.K., E.S.T., and R.D.S.) and the Department of Chemistry (P.K.W. and B.S.H.), Stanford University, Stanford, California 94305, and the Molecular Biology Institute (W.T.W.), University of California, Los Angeles, California 90024. Received June 11, 1979. This work was supported by grants from the National Institutes of Health (No. GM 18539 and GM 21149) and the National Science Foundation (No. PCM 75-20091); E.S.T. received predoctoral support from the National Science Foundation and the National Institutes of Health.

[‡] Present address: The Biological Laboratories, Harvard University, Cambridge, MA.

[§] Present address: Department of Microbiology and Molecular Biology Institute, University of California, Los Angeles, Los Angeles, CA 90024.

^{||} National Institutes of Health Research Career Development Awardee (GM 00284). Present address: Department of Chemistry and Institute of Molecular Biology, University of Oregon, Eugene, OR 97403.

^{||} National Institutes of Health Research Career Development Awardee (GM 00225).

¹ Abbreviations used: CP, major coat protein (gene 8 product) of the coliphage M13; PnA, parinaric acid (9,11,13,15-octadecatetraenoic acid); *cis*-PnA, 9,11,13,15-*cis,trans,trans,cis*-parinaric acid; *trans*-PnA, 9,11,13,15-*all-trans*-parinaric acid; DMPC, dimyristoylphosphatidylcholine.

from DMPC and CP by the cholate dilution method of Racker et al. (1975) as modified by Wickner (1976, 1977). Briefly, CP was incubated at 37 °C for 30 min in 1% sodium cholate and 0.1 M NaHCO₃ buffer, pH 8.5, at a final protein concentration of 2.0 mg/mL. Insoluble material (<10%) was removed by centrifugation. DMPC (Sigma Chemical Co.) was suspended by brief sonication (~30 °C) in potassium phosphate buffer (50 mM, pH 7.0) at 40 mg of phospholipid per mL. DMPC (100 μ L; 4 mg) was added to 250 μ L (0.4 mg) of protein solution. The clear solution was incubated at 22 °C for approximately 20 min and then diluted to 20 mL with potassium phosphate buffer equilibrated at 23 °C. Within 1 h at 23 °C, the diluted lipid-protein suspension became quite turbid, indicating vesicle formation. Vesicles were collected by centrifugation (30000g for 1 h) and resuspended to the original volume with potassium phosphate buffer. In some cases this washing was repeated in order to remove more of the cholate. Residual detergent, determined by using [¹⁴C]-cholate, was less than one cholate per eight CP, and subsequent washing did not reduce this value further. The results reported here are independent of detergent artifacts. Vesicles without coat protein were prepared in the same way. These vesicles are somewhat smaller than those prepared in the presence of coat protein (Wickner, 1977).

Incorporation of CP into lipid vesicles was verified by addition of 5–10 μ L of CP labeled with [³H]proline (~1 μ Ci/mL) or [³H]lysine (~10 μ Ci/mL) to the lipid-protein incubation mixture prior to dilution and centrifugation. Recovery of radioactivity in the final vesicle and supernatant fractions was compared. Alternatively, protein incorporation into vesicles was determined by comparison of tryptophan fluorescence in the supernatant and pellet of vesicles collected by centrifugation.

Parinaric acid was added as a concentrated ethanolic solution. The maximal ethanol concentration was 0.3%, and the maximal PnA concentration was 2 μ M, ca. one PnA per 200 DMPC molecules and three CP molecules. Fluorescence measurements were made in potassium phosphate buffer, pH 7.0, 100 mM, essentially as described by Sklar et al. (1977b). Excitation and emission wavelengths are given in each experiment.

In experiments to determine the PnA content of reconstituted vesicles, vesicles containing PnA were collected by centrifugation at 10 or 30 °C. One percent Triton X-100 was added to vesicle pellets, and the absorbance at 320–325 nm was used to determine PnA content. PnA content of supernatant solutions was determined fluorometrically in the presence of 400 μ g/mL sonicated DMPC. Additional details appear in the figure legends.

Phase-transition experiments were done as previously described (Sklar et al., 1977b). Polarization experiments were conducted by using a Spex fluorolog fluorometer fitted with Glan-Thomson UV transmitting polarizers. Temperature scans were conducted at rates no greater than 1 °C/min, and temperature was monitored by a thermocouple inserted directly in the cuvette.

Results

The fluorescence intensity of *cis*-PnA in DMPC vesicles as a function of temperature is given in the upper curve of Figure 1. An abrupt decrease in intensity is seen at the DMPC transition temperature of 23 °C. The effect of the addition of one CP per 40 DMPC molecules is shown in the lower curve. The major effect is a decrease in the intensity of the fluorescence in the low-temperature region where the pure bilayer is in the solid phase. The fact that the PnA intensities

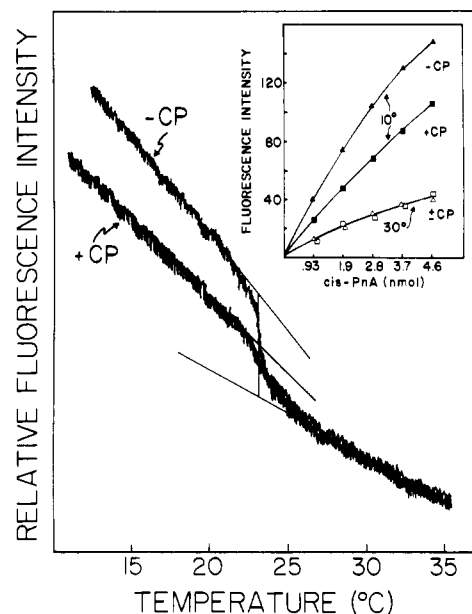


FIGURE 1: Phase transitions of DMPC vesicles in the presence (lower curve) and absence (upper curve) of CP were conducted as described under Materials and Methods. Each sample contained 2.1 μ mol of DMPC, 0.07 μ mol of CP (lower curve only), and 3.2 nmol of *cis*-PnA. The inset shows *cis*-PnA fluorescence in DMPC vesicles with (\square , \blacksquare) and without (Δ , \blacktriangle) CP at both 30 (\square , Δ) and 10 °C (\blacksquare , \blacktriangle). Conditions were the same as those described above.

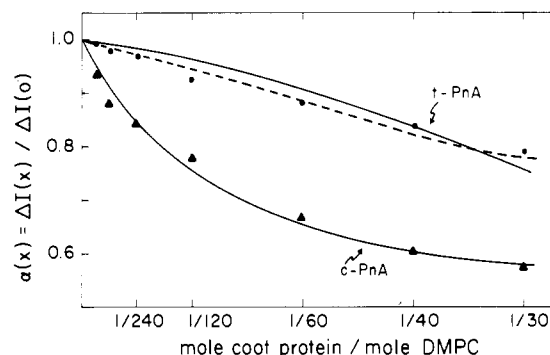


FIGURE 2: The change in transition amplitude as a function of coat protein concentration. Experiments were conducted as described in Figure 1. The coat protein concentration was varied as indicated, and the relative transition amplitude $\alpha(x)$ was determined with *cis*-PnA (\blacktriangle) and *trans*-PnA (\bullet). The curves are calculated by using eq 1 with $\sigma = 73.5$. The solid curve through the *cis*-PnA data used $\alpha_b = 0.55$ and $K = 0.73$. The dashed curve used $\alpha_b = 0.7$ and $K = 4$. The solid curve through the *trans*-PnA data used $K = 9.2$ with α_b fixed at 0.55.

are the same at high temperatures and different at low temperatures was confirmed by measurements of PnA fluorescence intensity at 10 and 30 °C for samples with and without coat protein. This is shown as the insert in Figure 1. The straight lines shown in Figure 1 were used to define an amplitude change, $\Delta I(x)$, the difference between the upper and lower lines at 22.5 °C, as a function of the ratio of CP to DMPC molecules, x . The ratio $\Delta I(x)/\Delta I(0)$ is plotted in Figure 2 as a function of x . The relative amplitude decrease observed by *cis*-PnA is much larger than that for *trans*-PnA.

The fluorescence emission and excitation spectra of CP incorporated into DMPC vesicles are shown in Figure 3. The absorption spectrum of *cis*-PnA is included to demonstrate the spectral overlap of the two chromophores (hatched area). The low wavelength of the CP tryptophan emission (330 nm) supports the conclusion (Wickner, 1976) that the tryptophan residue is located in a hydrophobic environment (Burststein et al., 1973). The spectra of Figure 3 in combination with the

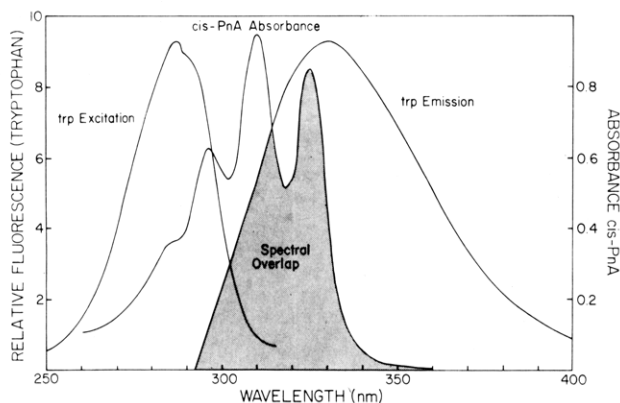


FIGURE 3: Excitation and emission spectra of coat protein in DMPC vesicles—spectral overlap with PnA absorbance. Fluorescence was measured at 330 nm (slit band-pass = 10 nm), and the wavelength of excitation was 286 nm (slit band-pass = 5 nm). Sample temperature was 10 °C. Absorbance of *cis*-PnA was measured in methanol at a concentration of approximately 3 $\mu\text{g/mL}$. The hatched region represents the area of spectral overlap.

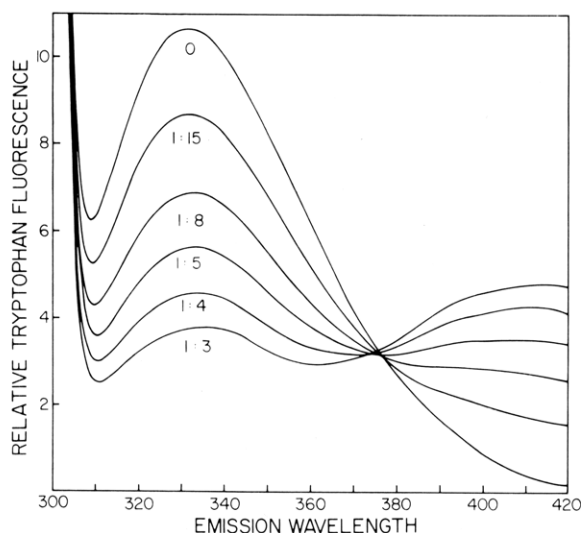


FIGURE 4: Quenching curves. Fluorescence emission spectra of DMPC-CP vesicles were recorded as described in the legend to Figure 3. Aliquots (2 μL) of a stock solution of *cis*-PnA (100 $\mu\text{g/mL}$ in ethanol) were added to 2 mL of vesicles resuspended at a final concentration of 300 $\mu\text{g/mL}$ DMPC and 30 $\mu\text{g/mL}$ CP. Numbers below each curve indicate the mole ratio of PnA/CP. Final PnA concentration was approximately 2 μM . The sample temperature was 30 °C.

results given previously (Sklar et al., 1977b) indicate that the spectral overlap integral J is roughly $190 \times 10^{-16} \text{ cm}^3 \text{ M}^{-1}$. The fluorescence quantum yield of the tryptophan in these vesicles is not known. Typical values for globular proteins are 0.1–0.4 (Burststein et al., 1973). A rough estimate of the value of the 50% energy transfer distance R can be obtained by using $K^2 = 2/3$ and $Q_d = 0.3$. This is $R_0 = 31 \text{ \AA}$. An upper limit for R_0 may be obtained by using $K^2 = 4$ and $Q_d = 1$. This is $R_0 < 49 \text{ \AA}$.

The effect of the addition of *cis*-PnA to these DMPC-CP vesicles is shown in Figure 4. The spectra show the decrease in the intensity of the tryptophan fluorescence upon addition of *cis*-PnA to CP-DMPC vesicles equilibrated at 30 °C. The lowest curve corresponds to a mole ratio of PnA/CP/DMPC of 1:3:220. The peak intensities from this figure are plotted in Figure 5 (as a quenching curve). In addition, the data for *trans*-PnA, also at 30 °C, are presented in Figure 5A. The results for *cis*-PnA and *trans*-PnA are identical for $T = 30$ °C where the bilayer is in the fluid state.

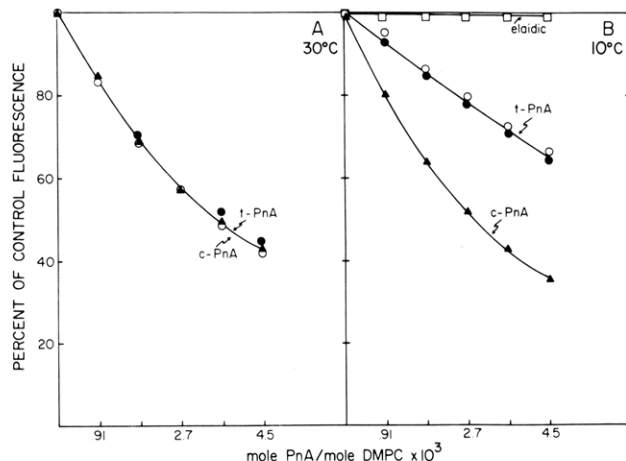


FIGURE 5: Decrease in CP fluorescence of DMPC-CP vesicles upon addition of PnA at 30 °C. (A) *trans*-PnA [(O) and (●) are duplicates] or *cis*-PnA (▲) was added to vesicles which contained 300 $\mu\text{g/mL}$ DMPC and 30 $\mu\text{g/mL}$ CP at 30 °C. Final PnA concentration was 0.5 $\mu\text{g/mL}$ (2 μM), which corresponds to a mole ratio of 1 PnA/3 CP/220 phospholipid molecules. Percent of control fluorescence was determined from emission curves recorded as described in the legends to Figures 3 and 4. (B) Decrease in CP fluorescence in DMPC-CP vesicles upon addition of PnA at 10 °C. *trans*-PnA (O), *cis*-PnA (▲), or elaidic acid (□) was added to samples containing 300 $\mu\text{g/mL}$ DMPC and 30 $\mu\text{g/mL}$ CP.

Table I: Fluorescence Quenching of M13 Coat Protein by Parinaric Acid at Various Molar Ratios of Protein to Lipid

| PnA/lipid | fluorescence quenching | | | | | |
|-----------|----------------------------|-------------------|-------------------|------------------------------|-------------------|-------------------|
| | <i>cis</i> -parinaric acid | | | <i>trans</i> -parinaric acid | | |
| | 1:120 ^a | 1:60 ^a | 1:30 ^a | 1:120 ^a | 1:60 ^a | 1:30 ^a |
| 30 °C | | | | | | |
| 1:1100 | 0.88 | 0.86 | 0.83 | 0.86 | 0.85 | 0.86 |
| 2:1100 | 0.77 | 0.76 | 0.71 | 0.77 | 0.74 | 0.76 |
| 3:1100 | 0.68 | 0.68 | 0.63 | 0.70 | 0.66 | 0.68 |
| 4:1100 | 0.61 | 0.62 | 0.56 | 0.64 | 0.59 | 0.61 |
| 5:1100 | 0.55 | 0.56 | 0.51 | 0.59 | 0.53 | 0.54 |
| 10 °C | | | | | | |
| 1:1100 | 0.82 | 0.83 | 0.83 | 0.91 | 0.92 | 0.92 |
| 2:1100 | 0.70 | 0.70 | 0.68 | 0.86 | 0.84 | 0.86 |
| 3:1100 | 0.63 | 0.62 | 0.57 | 0.80 | 0.78 | 0.75 |
| 4:1100 | 0.55 | 0.56 | 0.51 | 0.75 | 0.73 | 0.74 |
| 5:1100 | 0.50 | 0.52 | 0.47 | 0.72 | 0.69 | 0.68 |

^a Molar ratios of coat protein to lipid.

Quenching titrations were also carried out at 10 °C. As shown in Figure 5B, the quenching by *cis*-PnA is slightly more efficient at 10 °C than at 30 °C while *trans*-PnA is much less efficient at the lower temperature. Addition of elaidic acid has no effect.

A series of quenching curves were determined at different coat protein to lipid ratios in order to see if there was any association of the parinaric acid with the coat protein (Table I). A recent analysis of the effect of donor-acceptor association on the quenching curves (Wolber & Hudson, 1979) demonstrated that the quenching is very sensitive to the donor concentration if association is important. No evidence for such association was found since the quenching curves were essentially independent of CP concentration.

Tryptophan fluorescence intensity for CP-DMPC vesicles recorded as a function of temperature was determined for bilayers containing *cis*-PnA, *trans*-PnA, or no PnA as shown in Figure 6. Vesicles were equilibrated at 10 or 30 °C and 2 μM *cis*- or *trans*-PnA. The sample temperature was increased through the DMPC phase transition, and the tryptophan fluorescence intensity was recorded as a function of

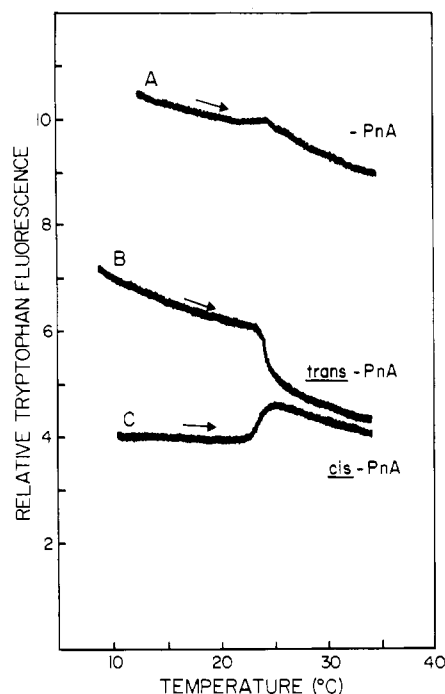


FIGURE 6: Temperature dependence of CP fluorescence in vesicles containing $2 \mu\text{M}$ PnA. Fluorescence at 330 nm (slit = 10 nm) was recorded during excitation at 286 nm (slit = 5 nm). Temperature was varied at the rate of approximately $1^\circ\text{C}/\text{min}$ by using a circulating water bath. Three heating curves are shown. Curve A shows CP fluorescence as a function of temperature in the absence of PnA. Curves B and C show CP fluorescence in the presence of *trans*- or *cis*-PnA, respectively. Mole ratios of PnA/CP/DMPC were approximately 1:3:220. The arrows indicate the direction of the temperature scan.

temperature. The fluorescence intensity of the coat protein alone decreased slightly with increasing temperature and showed a small discontinuity at the phase-transition temperature of 23°C . A striking decrease in the tryptophan fluorescence was observed in the vesicles containing *trans*-PnA upon heating through the DMPC phase transition. This indicates increased energy transfer in the fluid phase. The increase in tryptophan fluorescence in the presence of *cis*-PnA indicates a decreased transfer efficiency in the fluid phase. These curves are reversible and consistent with the fixed-temperature quenching curves of Figure 5.

One possible reason for the change in the PnA quenching efficiency as measured by tryptophan fluorescence changes at the DMPC phase transition is that there is a change in the amount of the polyene fatty acid acceptor chromophore in the bilayer. Decreased quenching efficiency of *trans*-PnA below 23°C (Figure 5B) could be due to a decreased association of *trans*-PnA with the bilayer. Conversely, *cis*-PnA might have decreased association with the vesicles above 23°C . This possibility was investigated by collecting the vesicles used in this experiment equilibrated with *cis*- and *trans*-PnA at 10 and 30°C . At 10°C it was found that 95% of the *trans*-PnA and 89% of the *cis*-PnA were pelleted with the vesicles. At 30°C the percentage of both *trans*-PnA and *cis*-PnA in the vesicles was 88%. This factor alone would result in an increased tryptophan fluorescence intensity rather than in the observed decrease. This minor redistribution of the polyene fatty acid between the vesicle and the buffer is small and will not be considered in subsequent discussion. Likewise, small changes in fluorescence quantum yield at different temperatures do not affect our interpretation of these results.

The polarization of the fluorescence of *trans*-PnA in DMPC bilayers is shown in Figure 7. The major effect of addition

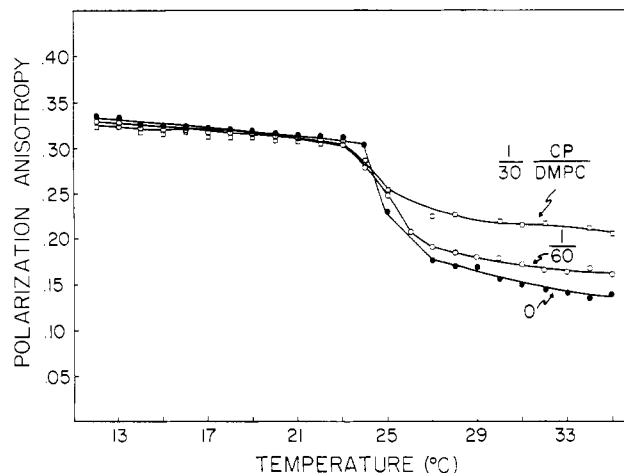


FIGURE 7: Polarization of PnA fluorescence in DMPC vesicles containing CP. The polarization of the fluorescence of *trans*-PnA was determined in DMPC vesicles containing no coat protein (\bullet), 1 CP/60 lipids (\circ), and 1 CP/30 lipids (\square). The data is presented as the fluorescence anisotropy, $r = (I_{\parallel} - I_{\perp}) / (I_{\parallel} + 2I_{\perp})$. Excitation was at 315 nm and emission was at 420 nm.

of CP is an increased polarization at temperatures above the phase transition. Similar results were obtained with *cis*-PnA.

Discussion

The experiments presented above suggest a model for the effect of coat protein on bilayer structure whose essential feature is that at 10°C the coat protein causes a disruption of the ordered gel phase. Several other conclusions can be drawn from these experiments. (a) The perturbation of the bilayer is spatially localized near the coat protein. (b) *trans*-PnA preferentially partitions into the bulk solid phase relative to the perturbed region. (c) The fluorescence intensity of *cis*-PnA in the perturbed region is lower than in the bulk solid phase. (d) Above the transition temperature of 23°C where the bulk bilayer is fluid, the effect of the coat protein on probe intensity and partitioning is small, but a significant decrease in probe rotational motion is observed. These conclusions do not depend on any assumptions concerning the spatial distribution of the coat protein in the bilayer. However, in order to provide a quantitative evaluation of these experiments, we have adopted a simple random distribution, annular domain model. According to this model, each CP is surrounded by an annulus of perturbed lipid. Within this annulus, the bilayer is imagined to have a uniform structure; outside the annulus, the bilayer is assumed to have the structure of the pure lipid at the same temperature. The proteins and their associated annuli are assumed to be randomly distributed in the bilayer so that their annuli may overlap. The purpose of the following discussion is to examine the quantitative agreement of this model with our data. We do not wish to imply that the model is unique, however, and consequently alternative interpretations of each experiment will be noted.

The experiments of Figure 1 show that the M13 CP has no effect on the PnA fluorescence intensity above the DMPC phase transition but that below the transition temperature the CP modifies the bilayer structure such that the PnA intensity is decreased. This results in a decrease in the transition amplitude with increasing CP content (Figure 2). The total intensity is the weighted sum of the annular and the bulk intensities, with the weighting factors being the mole fraction of the probe in the respective region. According to our random overlap model, the curvature in Figure 2 is due to overlap of the annular domains. With $\Delta I(x)$ as defined above and $\alpha(x)$

defined as the relative decrease in ΔI , i.e., $\alpha(x) = \Delta I(x)/\Delta I(0)$, then, according to the Appendix, we have

$$\alpha(x) = \alpha_b + K(1 - \alpha_b)/[K - 1 + \exp(x\sigma)] \quad (1)$$

The partition coefficient K is defined as the ratio of the concentration of the probe in the bulk lipid to the concentration in the annular lipid. We have included the possibility that the intensity of the probe in the annular region may be different for temperatures above and below the transition. The quantity α_b is the ratio of this annular intensity change to the bulk intensity change. The area of the annular region measured in units of area per phospholipid is designated σ . The product $x\sigma$ is, therefore, the fraction of the total lipid area that would be annular lipid if there were no overlap of the annular regions.

The three parameters of eq 1 were adjusted to give the best least-squares fit to the *cis*-PnA data of Figure 2. The curve is the resulting calculated fit. The value obtained for α_b is 0.55 ± 0.03 . This means that the intensity of the *cis*-PnA probe in the annular region extrapolated to 22.5 °C from the low-temperature (solid) region is approximately halfway between the solid bulk bilayer intensity and the fluid bulk bilayer intensity. The annular lipid undergoes a phase transition near 22.5 °C but with only 55% of the amplitude of pure lipid transition on this intensity basis.

The value of the parameter σ is 73.5 ± 2 . This means that each coat protein perturbs about 74 lipids when the bulk bilayer is in the solid phase. This corresponds to 37 lipids in each monolayer or three to four rings of lipid around the protein. This size parameter σ reflects the effective area of the annular lipid in terms of the tendency of the perturbed regions to overlap.

The *cis*-PnA intensity decrease associated with addition of the coat protein to the DMPC bilayer below 22.5 °C indicates that the annular region has a partially disordered structure, intermediate between that of the solid and fluid phases. It is known from other experiments (Sklar et al., 1977a, 1979) that the partition coefficient K for *cis*-PnA for coexisting solid and fluid phases is slightly less than unity (0.65 ± 0.2) (Sklar et al., 1979). The value obtained by fitting the *cis*-PnA data of Figure 2 was $K = 0.73 \pm 0.1$. This number by itself is not particularly significant, but it is important to note that adjustment of K does not result in appreciable changes in the parameters α_b and σ . For instance, the use of $K = 1$ results in optimized values of α_b and σ of 0.52 and 75.6.

A more important qualitative idea is that the disordered, fluidlike structure of the annular lipid should be reflected in a decreased affinity for *trans*-PnA relative to the bulk solid lipid. The partition coefficient for *trans*-PnA is known to be ~ 3 –4 in favor of solid with coexisting solid and fluid phases (Sklar et al., 1979). If the annular region is "fluidlike", then *trans*-PnA will partition into the bulk lipid and will not sense the presence of the coat protein in terms of the temperature dependence of its fluorescence intensity. This explains the difference between the *cis*- and *trans*-PnA curves of Figure 2 in qualitative terms and confirms the assignment of a relatively fluid structure to the annular region (relative to the solid phase) using a different criterion: the partitioning of *trans*-PnA rather than the intensity of *cis*-PnA fluorescence. The upper solid curve in Figure 2 is eq 1 using the same parameters as for the lower *cis*-PnA curve except that K is increased from 0.73 to 9.2. This involves adjustment of one parameter. A considerably improved fit to the data is obtained if the asymptotic value α_b is also allowed to vary. In this case, with σ fixed at 73.5, the optimum values are $\alpha_b = 0.7$ and $K = 4$ (dashed curve of Figure 2).

An alternative interpretation of the curvature of Figure 2

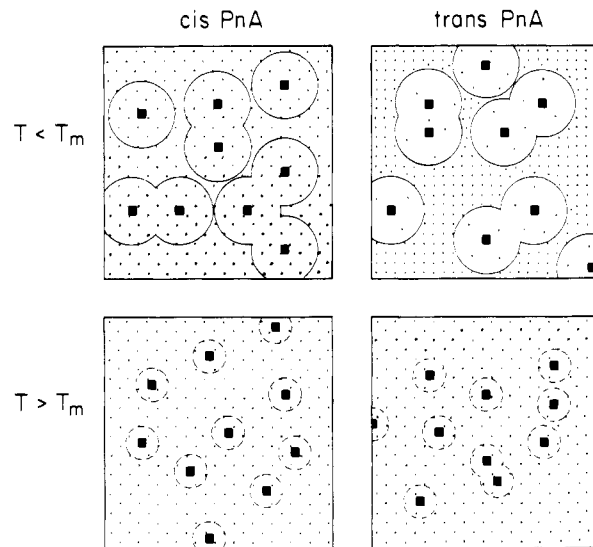


FIGURE 8: Diagrammatic representation of the lateral distribution of molecules in CP-DMPC vesicles. (■) represents CP molecules, (●) represents PnA molecules, the large circle represents annular lipid, and the white background represents bulk lipid. The representation of probe molecules does not indicate numbers of probe molecules relative to CP or DMPC but rather the density distribution under the indicated conditions. The smaller dashed circles surrounding the CP molecules for $T > T_m$ indicate uncertainty about the size and structure of this lipid.

is that it is related to lateral aggregation of the proteins. In this case the behavior at high CP concentration is related to the lipid content of the aggregated species rather than to the residual transition amplitude α_b . The slope near $x = 0$ is still related to the number of perturbed lipids in the nonaggregated state and is 70–90 lipids/coat protein.

According to either interpretation, the difference between the *cis* and *trans* curves of Figure 2 reflects a decrease in the fraction of the *trans* probe that is in a perturbed environment. The perturbed annular region is associated with the coat protein and, therefore, the *trans*-PnA distribution is not uniform with respect to the coat protein. A pictorial summary of the situation is given in Figure 8. The mean distance between the coat protein and a PnA is larger for *trans*-PnA than for *cis*-PnA below T_m . This difference in the spatial distribution of the two probes is reflected in the Förster energy transfer experiment based on the decreased tryptophan emission intensity observed on addition of *cis*- or *trans*-PnA. Since the characteristic energy transfer distances R_0 are similar for each pair, any difference in the quenching efficiency by the two acceptors will reflect differences in the spatial distribution.

The data of Figure 5A and Table I show that *cis*- and *trans*-PnA are equally efficient as energy acceptors for CP emission at 30 °C. The theory of Förster energy transfer in two dimensions (Fung & Stryer, 1978; Wolber & Hudson, 1979) was applied to this data, and it was found that the observed quenching is consistent with a random distribution and an energy transfer R_0 of 36–43 Å. This result was derived from the quenching experiment based on the assumption that the CP tryptophan is located at the center of the bilayer so that acceptors in both monolayers are equally effective quenchers. A value of 67 Å² was used for the area per phospholipid at 30 °C. The 36–43-Å value for R_0 is reasonable in view of the spectroscopic values given above.

The quenching curves obtained at 10 °C (Figure 5B) are quite different for *cis*- and *trans*-PnA. Most of the difference between the quenching by these two probes is due to the

structural change that occurs at the pure DMPC phase transition (Figure 6). The *cis*-PnA quenching is slightly more efficient at 10 °C than at 30 °C. This is due, in part, to the contraction of the bilayer at the phase transition and a corresponding increase in the acceptor density. However, there must also be a contribution from other factors such as a slight preferential partitioning into the region near the coat protein at low temperature, i.e., $K < 1$, as implied by the PnA intensity data.

The decreased quenching by *trans*-PnA at 10 °C is in qualitative agreement with the picture derived above from the PnA intensity data—i.e., the decreased quenching is due to the presence of an annular region with a lower relative affinity for *trans*-PnA. This can again be put on a quantitative basis by using the random annular model (Figure 8) as the basis for a simulation of the expected degree of energy transfer (Fung & Stryer, 1978; Wolber & Hudson, 1979). The value of R_0 is taken from the *cis*-PnA data, and the partition coefficient is taken to be 4. The only adjustable parameter is the annular radius. The value obtained by adjustment of this parameter to fit the *trans*-PnA data of Figure 5B corresponds to an annulus containing 70–100 DMPC molecules, 35–50 in each monolayer.

The decreased quenching by *trans*-PnA relative to *cis*-PnA at 10 °C could be due to a reduced R_0 associated with a relatively unfavorable orientation factor for *trans*-PnA. If this were the case, the orientation factor K^2 would have to be 20-fold smaller for *trans*-PnA than for *cis*-PnA. This is unlikely on structural grounds and is inconsistent with a random lateral distribution of acceptors, since this will result in a variable orientation factor.

This quenching data is also consistent with nonrandom coat protein distributions. For instance, the coat protein may exist in a distinct phase which has a reduced partition coefficient for *trans*-PnA. This protein-rich phase must have a considerable lipid content, however, since the quenching by *cis*-PnA is as efficient at 10 °C as at 30 °C.

The fluorescence intensity and quenching experiments discussed above do not provide much information concerning the effect of the coat protein on the fluid bilayer. In contrast, the fluorescence polarization data of Figure 7 reveal the effect of the CP on the properties of the fluid phase. These results demonstrate that above the phase transition the annular lipid has restricted orientational motion relative to the bulk fluid phase. These data are not sufficient to determine the combined factors of the extent of the annular region, the fluorescence quantum yield, the partition coefficient, and the polarization anisotropy of the probe in the annular region. These quantities can be separated by using nanosecond fluorometry. The small effect of CP on the intensity of PnA fluorescence above T_m and the apparent lack of differential quenching could be due to the small extent of the annular region rather than to a close structural similarity to the fluid phase.

The lack of a significant effect of the coat protein on the PnA polarization below T_m is due in part to the decreased fluorescence intensity of the probe in the annular region. The polarization anisotropy is weighted by the component intensities and is therefore weighted in favor of the bulk probe contribution. A detailed interpretation of the low-temperature polarization data must also await further nanosecond fluorometry experiments, which are in progress.

Conclusions

The picture that emerges from the experiments and analysis presented above is that the M13 coat protein disrupts the structure of the solid-phase DMPC bilayer, forming an annular

domain of 35–50 lipids in each monolayer which is “fluidlike” in terms of its relative affinity for the two isomers of parinaric acid and partially fluid in terms of the intensity of PnA fluorescence. These conclusions are consistent with the recent deuterium NMR studies of Oldfield et al. (1978) and with several studies of other proteins in pure lipids below their phase transition (Curatolo et al., 1978; van Zoelen et al., 1978; Chapman et al., 1977). The effect of the coat protein on the fluid-phase bilayer is a restriction of the orientational mobility of the acyl chains.

Three techniques were used in this study (PnA polarization, intensity, and energy transfer acceptance). Two of these techniques were combined with the differential partitioning of the two isomers of PnA. The analysis of PnA intensity changes at the DMPC thermal transition included the contribution from the melting of the annular lipid and the overlap of annular domains associated with a random distribution. The differential partitioning of *cis*- and *trans*-PnA into the annular lipid provides a new structural definition of this perturbed region. This probe behavior, in combination with Forster energy transfer from the protein, establishes that the perturbed lipid is, in fact, located near the protein.

Finally, it should be pointed out that, although the above analysis is a consistent interpretation of the data obtained from several techniques, it is not a unique interpretation. It is possible to construct a family of equally consistent interpretations of these experiments by postulating protein dimers or other small aggregates or by separating the protein with its lipid annular domain into a distinct phase. The restrictions imposed by our data are that there must be 70–80 lipids perturbed by each coat protein at low protein levels, these perturbed lipid regions must be near the protein, and the distribution of protein in the protein-rich domains must not significantly perturb the random distribution of lipid acceptors relative to the protein donors. This last restriction eliminates the possibility that the protein exists in large aggregates from which lipid is excluded. This ambiguity concerning the state of aggregation of the coat protein can be eliminated by performing nanosecond fluorescence lifetime and polarization experiments.

Appendix

The change in intensity at the phase transition, ΔI , defined by the construction in Figure 1 is the difference between the solid- and fluid-phase intensities extrapolated to the transition temperature. The intensity of the probe in the fluid phase, Q^F , is independent of the coat protein concentration. The intensity of the probe in the solid phase is the sum of the bulk and annular contributions. Thus

$$\Delta I = fQ_B^S + (1-f)Q_A^S - Q^F = f(Q_B^S - Q_A^S) + Q_A^S - Q^F \quad (A1)$$

where f is the fraction of the probe in the bulk lipid region and Q_A^S and Q_B^S are the intensities per unit of probe concentration in the annular and bulk regions when the bulk is solid. The quantity f is a function of the number of coat proteins per lipid, x . When there is no coat protein, $f = 1$ so $\Delta I(x = 0) = Q_B^S - Q^F$ and

$$\alpha(x) \equiv \Delta I(x)/\Delta I(0) = f(1 - \alpha_b) + \alpha_b \quad (A2)$$

where

$$\alpha_b \equiv (Q_A^S - Q^F)/(Q_B^S - Q^F) \quad (A3)$$

Formally, α_b is the relative intensity change which would be

observed when $f = 0$, i.e., all of the bilayer is annular.

The fraction of probe in the bulk lipid region is related to the probe partition coefficient, K , and the ratio of bulk to annular lipid area, R , by

$$f = KR/(1 + KR) \quad (A4)$$

The area of an individual annular domain in units of the area of a phospholipid is designated σ , i.e., $\sigma = a_A/a_L$. The mean number of coat proteins in a region of area a_A is $x\sigma$. According to Poisson statistics, the probability of finding an area of radius a_A which contains no coat proteins is $\exp(-x\sigma)$. Letting $a_A = \pi r_A^2$, it must be the case that the lipid at the center of the protein-free area is at least a distance r_A from the nearest coat protein and is therefore in the bulk phase. From this we have

$$R = e^{-x\sigma}/(1 - e^{-x\sigma}) = (e^{x\sigma} - 1)^{-1} \quad (A5)$$

Combining eq A5, A4, and A2 yields eq 1 of the text.

References

- Asbeck, F., Beyreuther, K., Kohler, H., von Wettstein, G., & Braunitzer, G. (1969) *Hoppe-Seyler's Z. Physiol. Chem.* 350, 1047.
 Berde, C. B., Hudson, B. S., Simoni, R. D., & Sklar, L. A. (1979) *J. Biol. Chem.* 254, 391.
 Burstein, E. A., Vendenkine, N. S., & Ivkova, M. N. (1973) *Photochem. Photobiol.* 18, 263.
 Chapman, D., Connell, B. A., Eliaz, A. W., & Perry, A. (1977) *J. Mol. Biol.* 113, 517.
 Chapman, D., Gomez Fernandez, J. C., & Boni, F. M. (1979) *FEBS Lett.* 98, 211.

- Curatolo, W., Verma, S. D., Sakura, J. D., Small, D. M., Shipley, G. G., & Wallach, D. F. H. (1978) *Biochemistry* 17, 1802.
 Fung, B., & Stryer, L. (1978) *Biochemistry* 17, 5241.
 Hagen, D. S., Weiner, J. H., & Sykes, B. D. (1978) *Biochemistry* 17, 3860.
 Knippers, R., & Hoffman-Berling, H. (1966) *J. Mol. Biol.* 21, 281.
 Oldfield, E., Gilmore, R., Glaser, M., Gutowsky, H. S., Hshung, J. C., Kang, S. Y., King, T. E., Meadows, M., & Rice, D. (1978) *Proc. Natl. Acad. Sci. U.S.A.* 75, 4657.
 Racker, E., Chein, T. F., & Kandrach, A. (1975) *FEBS Lett.* 57, 14.
 Sandermann, H., Jr. (1978) *Biochim. Biophys. Acta* 515, 209.
 Sklar, L. A., Hudson, B. S., & Simoni, R. D. (1975) *Proc. Natl. Acad. Sci. U.S.A.* 72, 1649.
 Sklar, L. A., Hudson, B. S., & Simoni, R. D. (1977a) *Biochemistry* 16, 819.
 Sklar, L. A., Hudson, B. S., & Simoni, R. D. (1977b) *Biochemistry* 16, 5100.
 Sklar, L. A., Miljanich, G. P., & Dratz, E. A. (1979) *Biochemistry* 18, 1707.
 Tecoma, E. S., Sklar, L. A., Simoni, R. D., & Hudson, B. S. (1977) *Biochemistry* 16, 829.
 van Zoelen, E. J. J., van Dijck, P. W. M., DeKruiff, B., Verkleij, A. J., & van Deenen, L. L. M. (1978) *Biochim. Biophys. Acta* 514, 9.
 Wickner, W. (1975) *Proc. Natl. Acad. Sci. U.S.A.* 72, 4749.
 Wickner, W. (1976) *Proc. Natl. Acad. Sci. U.S.A.* 73, 1159.
 Wickner, W. (1977) *Biochemistry* 16, 254.
 Wolber, P. K., & Hudson, B. (1979) *Biophys. J.* 28, 197.

Interaction of Local Anesthetics with *Torpedo californica* Membrane-Bound Acetylcholine Receptor[†]

Steven G. Blanchard, Janet Elliott, and Michael A. Raftery*

ABSTRACT: The effects of local anesthetics on the rate of the agonist-induced increase in ligand affinity of membrane-bound acetylcholine receptor from *Torpedo californica* were examined. The rate of the transition in receptor affinity was determined by following the time-dependent increase in inhibition of iodinated α -bungarotoxin binding caused by 1 μ M carbamylcholine. At concentrations below those that directly inhibited the binding of iodinated α -bungarotoxin, dibucaine increased the rate of the transition to a high-affinity state and tetracaine decreased this rate. The measured rate constants were $0.026 \pm 0.008 \text{ s}^{-1}$ in the presence and $0.010 \pm 0.002 \text{ s}^{-1}$ in the absence of dibucaine while tetracaine decreased the rate

to $0.006 \pm 0.002 \text{ s}^{-1}$ as compared to a control value of $0.012 \pm 0.003 \text{ s}^{-1}$. A parallel was observed between the effectiveness of a compound in increasing or decreasing the rate of the agonist-induced transition in affinity and the change in its apparent inhibition constant in the presence of carbamylcholine (increase or decrease) measured by the displacement of tritiated perhydrohistrionicotoxin. This parallel could be explained by assuming (a) that local anesthetics bound directly to the specific histrionicotoxin binding site or (b) that they bound to a different site and the observed effects were caused by conformational changes.

The release of acetylcholine at the neuromuscular junction results in a transient depolarization of the postsynaptic membrane. This response is mediated by nicotinic acetylcholine

receptors (AcChR)¹ in this membrane and is considered to involve the binding of AcCh followed by a transient increase in membrane conductance. The ligand binding properties of the AcChR have been studied in vitro by using membrane fragment preparations enriched in this molecule obtained from several species of marine electric ray (Cohen et al., 1972;

[†] From the Church Laboratory of Chemical Biology, Division of Chemistry and Chemical Engineering, California Institute of Technology, Pasadena, California 91125. Received February 15, 1979. Contribution No. 5970. Supported by U.S. Public Health Service Grant NS10294, by a grant from the Muscular Dystrophy Association of America, and by Grant RR07003 awarded by the Biomedical Research Support Grant Program, Division of Research Resources, National Institutes of Health.

¹ Abbreviations used: AcChR, acetylcholine receptor; [¹²⁵I]- α -BuTx, α -bungarotoxin iodinated with ¹²⁵I; carb, carbamylcholine; H₁₂-HTX, perhydrohistrionicotoxin; PAA, procaine amide azide.